Int J Biometeorol (2014) 58:931–940
DOI 10.1007/s00484-013-0676-5

ORIGINAL PAPER

WSR-88D doppler radar detection of corn earworm moth migration

J. K. Westbrook · R. S. Eyster · W. W. Wolf

Received: 13 September 2012 / Revised: 29 April 2013 / Accepted: 29 April 2013 / Published online: 9 June 2013

Abstract Corn earworm (Lepidoptera: Noctuidae) (CEW) populations infesting one crop production area may rapidly migrate and infest distant crop production areas. Although entomological radars have detected corn earworm moth migrations, the spatial extent of the radar coverage has been limited to a small horizontal view above crop production areas. The Weather Service Radar (version 88D) (WSR-88D) continuously monitors the radar-transmitted energy reflected by, and radial speed of, biota as well as by precipitation over areas that may encompass crop production areas. We analyzed data from the WSR-88D radar (S-band) at Brownsville, Texas, and related these data to aerial concentrations of CEW estimated by a scanning entomological radar (X-band) and wind velocity measurements from rawinsonde and pilot balloon ascents. The WSR-88D radar reflectivity was positively correlated (r^2=0.21) with the aerial concentration of corn earworm-size insects measured by a scanning X-band radar. WSR-88D radar constant altitude plan position indicator estimates of wind velocity were positively correlated with wind speed (r^2=0.56) and wind direction (r^2=0.63) measured by pilot balloons and rawinsondes. The results reveal that WSR-88D radar measurements of insect concentration and displacement speed and direction can be used to estimate the migratory flux of corn earworms and other nocturnal insects, information that could benefit areawide pest management programs. In turn, identification of the effects of spatiotemporal patterns of migratory flights of corn earworm-size insects on WSR-88D radar measurements may lead to the development of algorithms that increase the accuracy of WSR-88D radar measurements of reflectivity and wind velocity for operational meteorology.

J. K. Westbrook (✉) · R. S. Eyster · W. W. Wolf
Areawide Pest Management Research Unit, USDA-ARS,
2771 F & B Road, College Station, TX 77845-4966, USA
e-mail: john.westbrook@ars.usda.gov

Keywords Insect · Biometeorology · Aerobiology · Aeroecology · Dispersal

Introduction

Airborne biota often produce substantial clear-air echoes on weather radar displays and can be quantified by the amount of radar-transmitted electromagnetic energy reflected by individuals and distributed biota (Chilson et al. 2012a). Radar reflectivity of biota such as insects (Nieminen et al. 2000), birds (Gauthreaux and Belser 1998; Larkin et al. 2002), and bats (Horn and Kunz 2008) may appear similar to that of precipitation. In addition to contributing to radar reflectivity, airborne organisms can act as tracers of radar-derived wind velocity (Achtemeier 1991; Wilson et al. 1994), which has proven useful for atmospheric forecasting of convective precipitation (Rennie et al. 2011). However, flying organisms can also alter radial velocity values measured by Doppler weather radars and wind velocity values measured by radar wind profilers (Jain et al. 1993; Miller et al. 1997; Gauthreaux et al. 1998).

A national network (NEXRAD) of S-band (10-cm wavelength) WSR-88D Doppler weather radars (Crum and Alberty 1993) provides nearly complete coverage of the US. WSR-88D radar measurements include reflectivity, radial velocity, and spectrum width (a measure of velocity variance), which are measured to a maximum range of 460, 230, and 230 km, respectively. WSR-88D radars complete a volume scan (or volume coverage pattern, VCP) of azimuthal sweeps at several elevation angles every 5–6 min in precipitation mode (VCP 11 or VCP 21), and every 10 min in clear-air mode (VCP 31 or VCP 32). Radar reflectivity algorithms are based on assumptions that spherical water droplets of known radius fill the range interval volume of the radar beam, and the droplet radius is less than one-tenth of the radar wavelength to satisfy Rayleigh's law for the scattering of electromagnetic

radiation by the droplets. Chilson et al. (2012a) noted that WSR-88D radars measure energy reflected by insects and other bioscatterers, but operational algorithms remove most of this information from visual presentation of the precipitation patterns. Comprehensive descriptions are available for WSR-88D data products (Klazura and Imy 1993) and Doppler radar theory (Doviak and Zrnic 1984; NOAA 1990).

Various deployed forms of X-band (3-cm wavelength) radars have been used effectively in entomological studies for several decades (Reynolds 1988; Chapman et al. 2011). Radar entomological measurements have been especially useful for detecting high-altitude nocturnal flight of insects (Wolf et al. 1995). Scanning entomological radars have been used to construct vertical profiles of aerial abundance of insects and estimate insect air speed and heading (Feng et al. 2008, 2009). Further, nightly and seasonal periodicity of the vertical profile of insect abundance has been monitored by vertically oriented radars (Beerwinkle et al. 1993; Wood et al. 2006), which frequently detect dense layers of insects at altitudes where winds maximize horizontal displacements. Radar cross-sections of individual corn earworm (CEW) moths [*Helicoverpa zea* (Boddie)] and other insects have been measured in the laboratory for use in classifying radar-detected insects based on body length and width (Riley 1985; Wolf et al. 1993; Hobbs and Aldhous 2006). Vertically-oriented radar systems that classify airborne insects based on insect mass, air speed, body length, body width, and wing-beat frequency have been developed in Australia (Dean and Drake 2005) and the UK (Smith and Riley 1996; Chapman et al. 2003). Automated vertically-oriented radars have continuously recorded long-term seasonal flight activity patterns of insects (including species of the Noctuidae family) from which several important hypotheses of insect migration have been tested (Chapman et al. 2010, 2012).

The timing and concentration of CEW moth emergence depends largely on the abundance and phenological stage of host plants. Raulston et al. (1992) determined that 1 billion to 7 billion CEW moths emerge annually from 2,000 km^2 of irrigated corn during the fruiting stage in the Lower Rio Grande Valley (LRGV) of northeastern Mexico and southern Texas. Airborne concentrations of insects detected by scanning X-band radar compared well with the estimated emergence and airborne flux of CEW moths from fields of host crops in the LRGV (Wolf et al. 1995). A substantial increase in the number of CEW moths in the atmospheric boundary layer typically begins at about 0.5 h after sunset and attains a maximum value about 1 h after sunset. Subsequently, the number of airborne CEW declines until ending at approximately 0.5 h before sunrise (Wolf et al. 1986). CEW and other noctuid moth species are typically distributed within the lowest 1,000 to 2,000 m above ground level (AGL) of the atmosphere, and may congregate within concentrated layers and orient toward a collective heading (Wolf et al. 1995).

Three to four generations of CEW are produced annually in the south-central US. Emergence of CEW moths from pupae occurs typically during a period of 10–14 days during late spring and early summer in the south-central US. Warm, dry conditions and synchronous planting of corn further constrain the duration of the moth emergence cycle. Insect phenological life cycles are similar in other temperate regions of the US, but are more confined to summer months. Algorithms developed for CEW in the LRGV could be useful in other geographic regions where night-flying insects are prevalent, provided the local flight phenology is known.

A study was conducted to examine the application of WSR-88D reflectivity, radial velocity, and spectrum width measurements to estimate aerial concentration and air speed of CEW migrating from fields during periods of peak emergence and emigration in the LRGV of Texas and northeastern Mexico. The objectives of this research were to quantify: (1) the relationship between WSR-88D reflectivity values and the airborne concentration of CEW-size insects; and (2) the relationship between WSR-88D radial velocity and spectrum width values and the flight velocity of CEW-size insects.

Methods

Native vegetation in the LRGV is comprised mostly of mesquite, chapparal, prickly pear cactus, and bunch grasses. Irrigation has allowed more than one-third of the LRGV to be cultivated for the production of corn, cotton, sorghum, citrus, and other fruit and vegetable crops (Orton et al. 1967). Corn is grown on approximately 2,000 km^2 of irrigated land in the LRGV.

NEXRAD WSR-88D data files for Brownsville, Texas (KBRO) were downloaded from the National Oceanic and Atmospheric Administration (NOAA) National Climatic Data Center (NCDC) website and stored on a 2-TB hard drive. Compressed data files for the time periods of 0000–0700 hours Universal Coordinated Time (UTC) and 0800–1500 hours UTC were downloaded for the active field research period of 4 June 1996–19 June 1996. The NOAA Weather and Climate Toolkit was downloaded from the NCDC Web site (http://www.ncdc.noaa.gov/oa/wct/) and used to decode the WSR-88D data files into three data fields [reflectivity (REF), radial velocity (VEL), and spectrum width (SPW)] as point files. Note that the use of the term 'radar reflectivity' used here is actually referred to as 'radar reflectivity factor' by Chilson et al. (2012c), and is a parameter that has been derived based on an assumption of uniformly distributed water droplets in the radar detection (range interval) volume. Each radar volume scan was processed three times to extract each data field. The decoding program was executed in a batch process to extract data from 0000–1200 hours UTC.

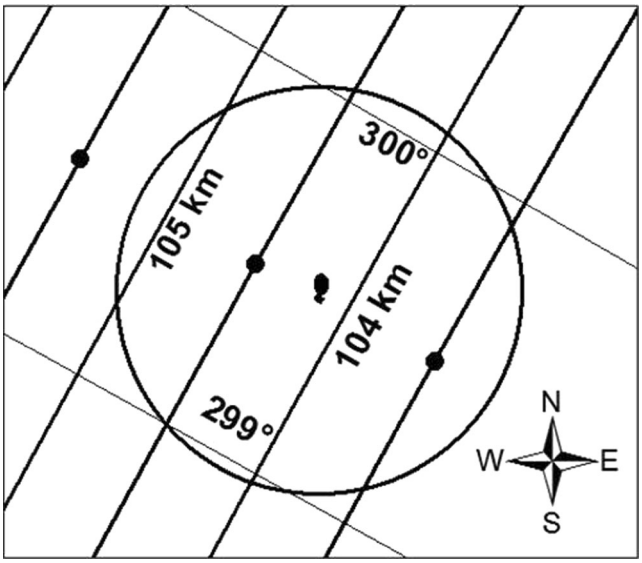

Fig. 1 Plan view of a 1-km radius measurement zone for extracting data from range interval volume centerpoints of WSR-88D radar elevation scans

Geographic coordinates of the WSR-88D S-band radar and a mobile, scanning X-band radar were registered on a map layer in ArcGIS V10.1 (ESRI, Redlands, CA). The WSR-88D beam width and beam height at three USDA-ARS field locations were calculated based on respective distances from the WSR-88D radar using the rdrhgt.exe program (Barker 1994).

A 1-km-radius measurement zone (Fig. 1) was created around each USDA-ARS field location to match the approximate maximum range for detection of individual CEW moths by the X-band radar. Data for all centerpoints of WSR-88D range interval volumes located within the measurement zones were selected for statistical analysis. All elevation angles (i.e., sweeps) in a WSR-88D volume scan were sampled and statistics were computed for each sweep. The REF values were compared to the discrete counts of targets observed by the X-band radar. The nightly pattern and daily maximum values of REF and discrete counts of targets were compared for similarity. The VEL values were compared to the wind velocity values calculated from pilot balloons tracked by theodolite at X-band radar sites and at Moore Air Base near Mission, Texas. A confounding situation existed for the radar comparisons. The WSR-88D data were valid at the centerpoint of each range interval volume. A series of range interval volumes of 1-km length for REF and 250-m length for VEL or SPW comprise the conical radar beam along each one-degree radial of the azimuthal scan. The distance from the WSR-88D to the X-band radar resulted in large beam widths of the WSR-88D range interval volumes. As a result, only a few WSR-88D range interval volumes were selected for each X-band radar location.

A scanning X-band radar, described by Wolf et al. (1995), was operated in June 1996 near Donna and Hargill, Texas, in the vicinity of the WSR-88D radar installation at Brownsville, Texas (KBRO) (Fig. 2). The X-band radar transmitted at a frequency of 9.45 GHz and peak power of 25 KW. A 1.2-m-diameter parabolic dish antenna was used to create a 1.2° radar beam width. A 1.7-kHz pulse repetition frequency and 250-ns pulse length facilitated radar detection of individual CEW-size insects to a distance of 1.8 km. Aerial concentrations of CEW-size insects were estimated from the X-band radar measurements by dividing the number of insects within an annulus on the plan position indicator (ppi) display by the annular detection volume. The counting annulus was defined by the X-band radar detection volume from a range of 1,210 to 1,400 m at each of eight elevation scans from 4° to 65°. Concentrations of individual CEW-size insects were recorded to a maximum altitude of 1,200 m. Aerial insect concentration data from the X-band radar were linearly interpolated to 100-m intervals for analysis.

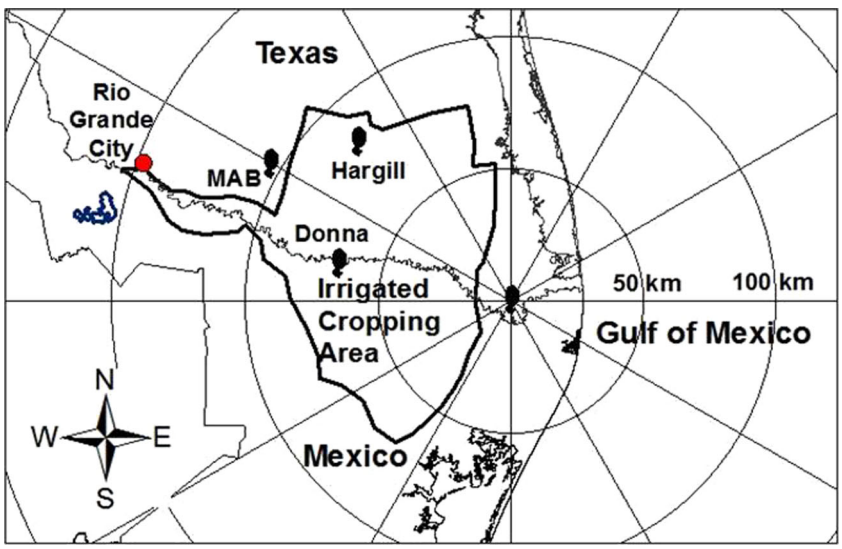

Fig. 2 Map of the Brownsville, Texas, WSR-88D radar (KBRO) coverage and USDA-ARS field locations at Moore Air Base (MAB), Donna, and Hargill in the Lower Rio Grande Valley (LRGV)

Vertical profiles of wind velocity were measured at Moore Air Base (MAB) by tracking pilot balloons using one of three methods: optical theodolite (Warren-Knight, Philadelphia, PA), optical theodolite with a radiosonde receiver (A.I.R., Woburn, MA), or scanning radar. Azimuth angles and elevation angles were smoothed by an 11-point, centered, moving-average scheme. Three-dimensional trajectories of the pilot balloons were calculated from the smoothed azimuth angles, elevation angles, and pilot balloon ascent rates. Wind velocity values were calculated as the time rate of change of the individual horizontal coordinates of the pilot balloons. Values of wind velocity nearest to intervals of 50 m AGL were output for subsequent statistical analysis.

Mean and maximum WSR-88D reflectivity values within 1-km measurement zones from the lowest two elevation scans (0.5° and 1.5°) at Donna, Hargill, and MAB were output at nearly coincident X-band radar scan times. Insect concentration values (i.e., number of CEW-size insects per detection volume) were derived from the X-band radar measurements. WSR-88D reflectivity values were regressed with values of insect concentration estimated for the altitude of the WSR-88D radar beam centerline (Table 1) and for the mean concentration throughout the beam width using PROC REG of the SAS version 9.2 statistical software (SAS Institute, Cary, NC).

Mean and maximum WSR-88D radial velocity values within 1-km measurement zones from the 0.5° elevation scan were output at nearly coincident pilot balloon and rawinsonde profile times. WSR-88D constant altitude plan position indicator (CAPPI) estimates of wind speed and wind direction were regressed with wind speed and wind direction measured by rawinsondes using PROC REG of the SAS version 9.2 statistical software (SAS Institute). Regressions were tested for significance ($P \leq 0.05$) using the Pearson correlation coefficient.

Results

WSR-88D reflectivity maps indicated patterns of aerial abundance of CEW-size insects in the LRGV in June 1996. For

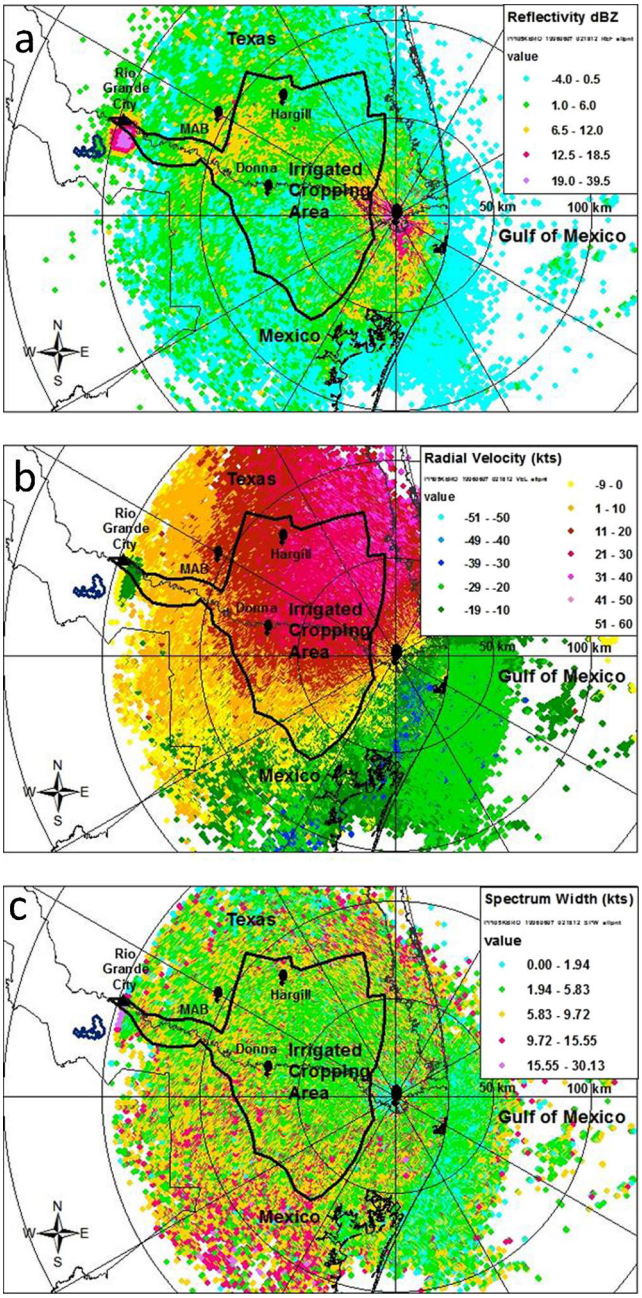

Fig. 3 Plan position indicator display of (**a**) reflectivity, (**b**) radial velocity, and (**c**) spectrum width observed in the 0.5°-elevation scan of the WSR-88D Doppler radar KBRO at Brownsville, Texas, at 0218 hours UTC (approximately 0.9 h after sunset) on 7 June 1996

Table 1 Description of Brownsville (KBRO), Texas, WSR-88D radar beam configuration at three USDA-ARS field sites in the Lower Rio Grande Valley (LRGV), Texas, in June 1996

Location	Position relative to KBRO WSR-88D radar			
	Range (km)	Azimuth (degrees)	Beam centerline altitude (m MSL)	
			at 0.5° elevation	at 1.5° elevation
Donna, Texas	67	281	854	2,028
Hargill, Texas	84	315	1,143	2,603
Moore Air Base (MAB), Texas	105	298	1,562	3,391

example, the WSR-88D often detected a cluster of maximum reflectivity (Fig. 3a), which originated over the irrigated crop production area in the LRGV at approximately 0.5 to 1.0 h after sunset and displaced downwind toward the northwest. At approximately 150 km west of the WSR-88D, there was a pronounced reflectivity maximum that was likely associated with bats departing from a roost near a lake in Mexico several kilometers south of Rio Grande City, Texas. The temporal pattern of mean WSR-88D reflectivity matched two characteristic features of the pattern of aerial insect concentration during peak emergence of CEW from fruiting corn per previous entomological radar investigations. First, mean WSR-88D reflectivity increased rapidly from sunset to about 1 h after sunset, then decreased monotonically until sunrise (Fig. 4). Second, mean WSR-88D reflectivity generally decreased from 4 to 19 June 1996 (Fig. 5a), which apparently corresponded with the second half of an approximately sigmoidal CEW emergence cycle.

The plan position indicator display of radial velocity (Fig. 3b) shows a cluster of inbound (northwesterly) flow associated with the suspected colony of bats detected by radar reflectivity (Fig. 3a). The areal presentation of spectrum width (Fig. 3c) generally indicates minimum values of spectrum width appear along the axis of the prevailing southeasterly flow, and maximum values of spectrum width appear along axes at approximately ±45° from the prevailing southeasterly flow. Low spectrum width values associated with the suspected bats located 150 km west of the WSR-88D suggest collective flight direction.

A CAPPI polar plot of WSR-88D radial velocity, spectrum width and reflectivity is shown for the WSR-88D volume scan at 1:46 UTC on 5 June 1996 (Fig. 6). The overall wind direction appeared to be from 112°. The negative (in-bound) WSR-88D radial velocity values were maximum at 120° and positive (out-bound) velocities were maximum at 285°. The spectrum width was generally minimum at 135° and 315° and maximum at 225° and 45°. Higher WSR-88D reflectivity values were indicated at 135° and 315° and lower values at 225° and 45°. The superposition of the WSR-88D radar data here revealed an inverse relationship between spectrum width and reflectivity. These results suggest that airborne insects may have been aligned toward 45°, which was perpendicular to the prevailing wind direction.

A similar temporal pattern of radial velocity (Fig. 5b) was evident at the three USDA-ARS field locations in the LRGV. Radial velocity values were maximum at Hargill which is aligned closer to the prevailing wind direction. Mean velocity values exceeded 20 kts (10.3 m s^{-1}) on more than half of the nights from 4 to 19 June 1996. Passage of a cold front on the night of 8 June 1996 was the only occurrence of an inbound (northwesterly) wind. Spectrum width values generally ranged from 5 to 10 kts (2.6 to 5.1 m s^{-1}) (Fig. 5c). Spectrum width values were highest at Hargill when the associated radial velocity values were relatively low, yet spectrum width values were highest at Moore Air Base when radial velocity values were highest. These conditions at Hargill may be the result of more random motion when wind speeds are low and flight is over cropped areas. At MAB, the beam width (sample volume) is very large and may encompass varying wind velocities with altitude. This would result in a large standard deviation (spectrum width) of velocity.

X-band radar measurements of insect concentration at Donna and Hargill explained 21 % of the variance of radar reflectivity ($F_{1,130}=35.36$, $P\leq 0.0001$). The root mean square error (RMSE) for the regression fit of mean reflectivity equaled 4.2 dBZ. A positive log-log regression between the aerial concentration of CEW-size insects and WSR-88D reflectivity (expressed as a log-transformed

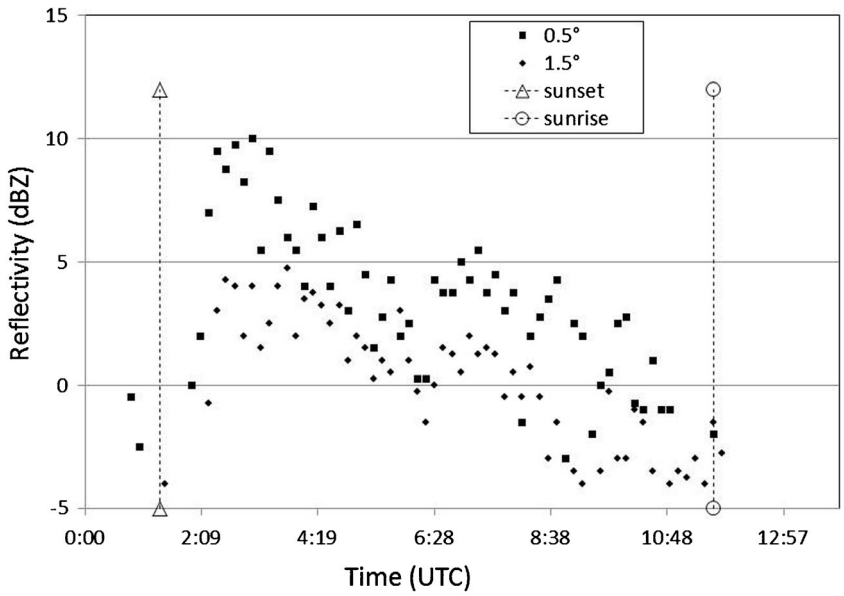

Fig. 4 Nocturnal time series of mean WSR-88D reflectivity (KBRO 0.5°- and 1.5°-elevation scans) at Moore Air Base, Texas, on 7 June 1996

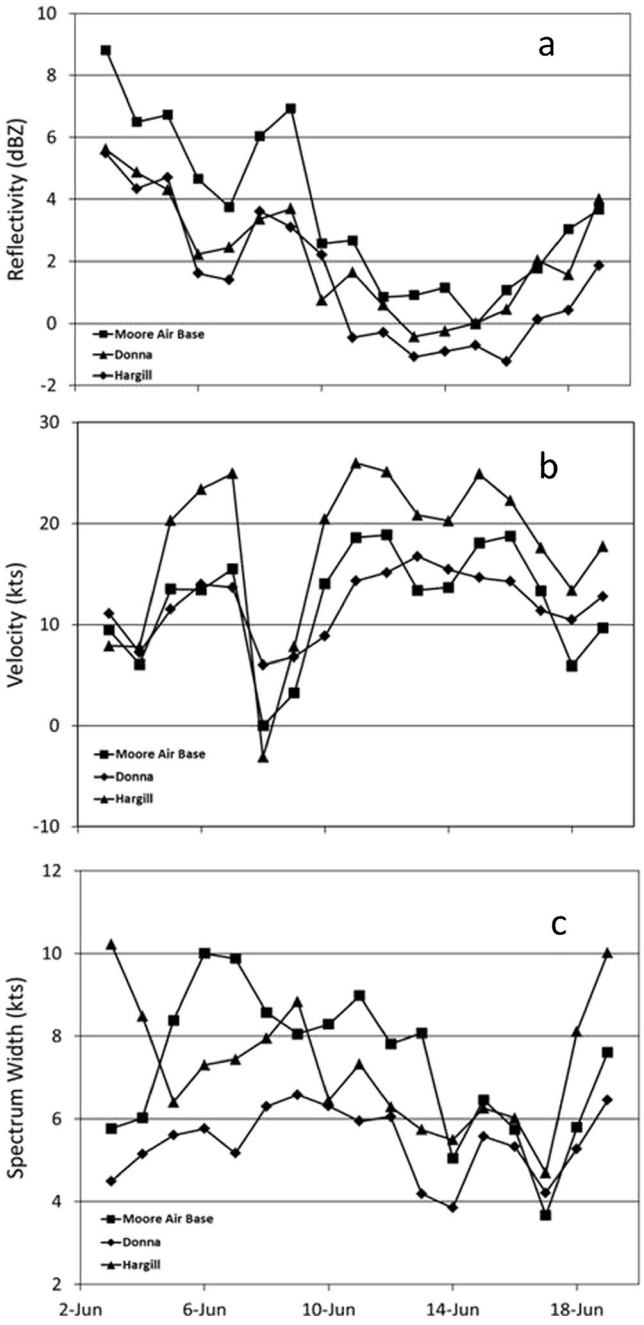

Fig. 5 Nightly (**a**) mean reflectivity, (**b**) radial velocity, and (**c**) spectrum width (WSR-88D Doppler weather radar KBRO at 0.5°-elevation scan) for Moore Air Base, Hargill, and Donna, Texas, on 4–19 June 1996

value, dBZ) is apparent (Fig. 7). The relatively low correlation between aerial concentration of insects and WSR-88D reflectivity may be due to subjective thresholding of targets displayed on the X-band radar plan position indicator based on the relative detectability, reflected image size, and air speed of biota in the counting annulus. Also, the WSR-88D radar beam may have detected CEW in the lowest 100–200 m of the atmosphere, below the estimated minimum altitude of the radar beam of the 0.5° elevation scan.

Results of the regression between WSR-88D CAPPI wind speed and the wind speed values measured by rawinsondes are presented in Fig. 8. Wind speed measured by rawinsondes explained 56 % of the variance of WSR-88D CAPPI estimates of wind speed ($F_{1,446}=562.43$, $P\leq 0.0001$). The RMSE for estimating WSR-88D CAPPI wind speed equalled 2.0 m s^{-1}. The RMSE value is reasonable because mean CEW air speed has previously been estimated as 4.5 m s^{-1} derived from successive locations of individual insects using a scanning, X-band radar (Westbrook et al. 1994). Further, RMSE values of WSR-88D CAPPI estimates of wind speed are expected to be maximum when the radial direction of the radar beam is aligned with a collective insect flight heading, and minimum when the beam is orthogonal to the collective heading. Wind direction measured by rawinsondes explained 63 % of the variance in WSR-88D CAPPI estimates of wind direction (Fig. 9). The RMSE for WSR-88D CAPPI wind direction was 12.6°.

A time-height graph of wind velocity measurements shows close similarity in the magnitude and direction of wind speed measured by pilot balloons and rawinsondes and estimated by CAPPI analysis of WSR-88D radial velocity (Fig. 10). The mean spectrum width values measured by the WSR-88D are posted above each WSR-88D wind vector. We assumed that the wind velocity at a selected altitude is constant across the entire area from MAB to KBRO when estimating wind velocity from the CAPPI data.

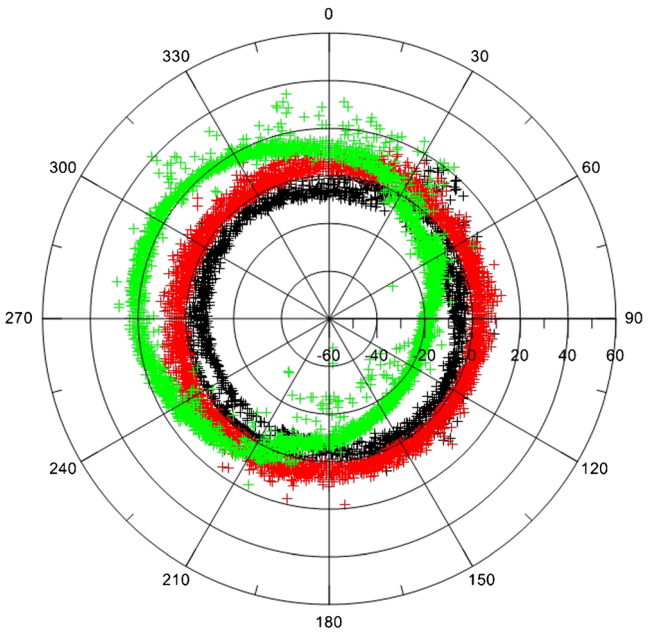

Fig. 6 Constant-altitude plan position indicator (CAPPI) plot of radial velocity (kts) (*green*), spectrum width (kts) (*red*), and reflectivity (dBZ) (black) at 600 m altitude measured by the WSR-88D radar at Brownsville, Texas, at 1:46 UTC (0.4 h after sunset) on 5 June 1996

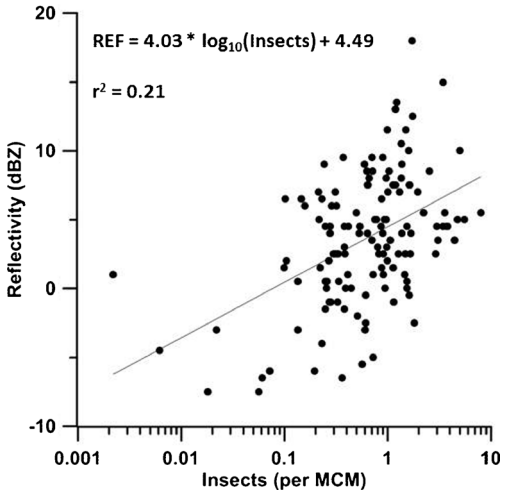

Fig. 7 Regression of WSR-88D reflectivity (0.5°-elevation scan) and aerial concentration of corn earworm-size insects [number per million cubic meters (MCM)] detected by a scanning X-band radar in the LRGV, Texas, in June 1996

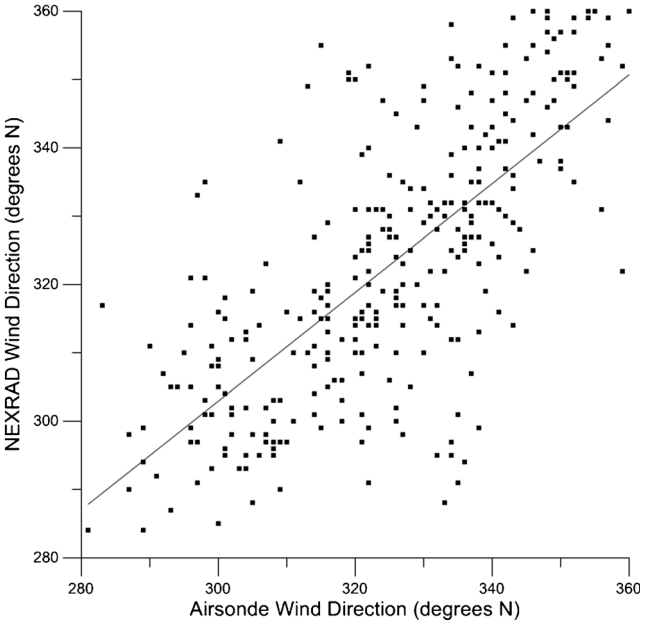

Fig. 9 Regression of WSR-88D CAPPI wind direction and rawinsonde wind direction from 200 to 1,200 m AGL for wind speed values ≥5 m s^{-1} at Moore Air Base, Texas, from 4 to 14 June 1996

Discussion

WSR-88D Doppler weather radars demonstrate the potential to estimate the aerial concentration and movement of night-flying insects over large areas such as crop production areas. Areawide surveillance by the NEXRAD network of WSR-88D radars creates opportunities for aeroecological investigations spanning time scales from hours to decades and spatial scales of hundreds of kilometers. Immediate agricultural application of WSR-88D radar data products is anticipated for identification of localized populations of emigrant CEW and estimation of migration pathways (Westbrook and Eyster 2003). Such radar-derived information of CEW migrations could efficiently direct pest management resources where and when needed to reduce massive emigration flights and alert crop producers and pest managers about the risk of infestations by migrant CEW.

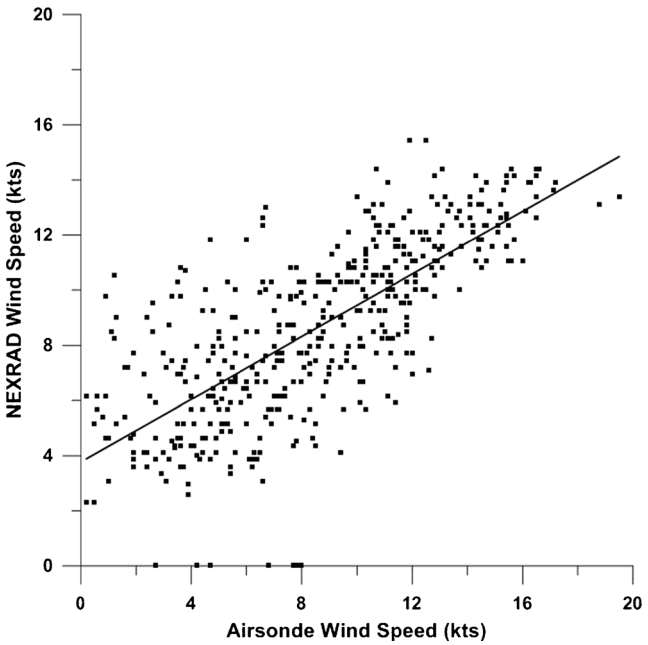

Fig. 8 Regression of WSR-88D CAPPI wind speed versus rawinsonde wind speed at Moore Air Base, Texas, from 4 to 14 June 1996

WSR-88D radars can detect bats (Horn and Kunz 2008), birds (Gauthreaux and Belser 1998) as well as insects during peak episodes of nightly flight, and parallel developments in the quantification of bird migration in Europe using C-band Doppler weather radar have been initiated (Dokter et al. 2011). Combining WSR-88D reflectivity, radial velocity, and spectrum width values will help to distinguish among biota. If radar cross-section data are available for a particular species and the species' population dynamics and flight periodicity is known or assumed, the aerial concentration of the species can be estimated from the radar reflectivity (Chilson et al. 2012c). Air speed of airborne biota is an important factor in distinguishing insects from birds and bats. Further investigation is needed to determine if spectrum width data can enhance the capability of WSR-88D radars to distinguish among biota. Improved capability to discriminate target species is expected when the WSR-88D has a dual-polarimetric option (Zrnic and Ryzhkov 1998a, 1998b; Chilson et al. 2012b).

Early-evening radar reflectivity patterns may identify geographic locations (e.g., a specific corn field) as sources of abundant emigration, and contribute to strategic management

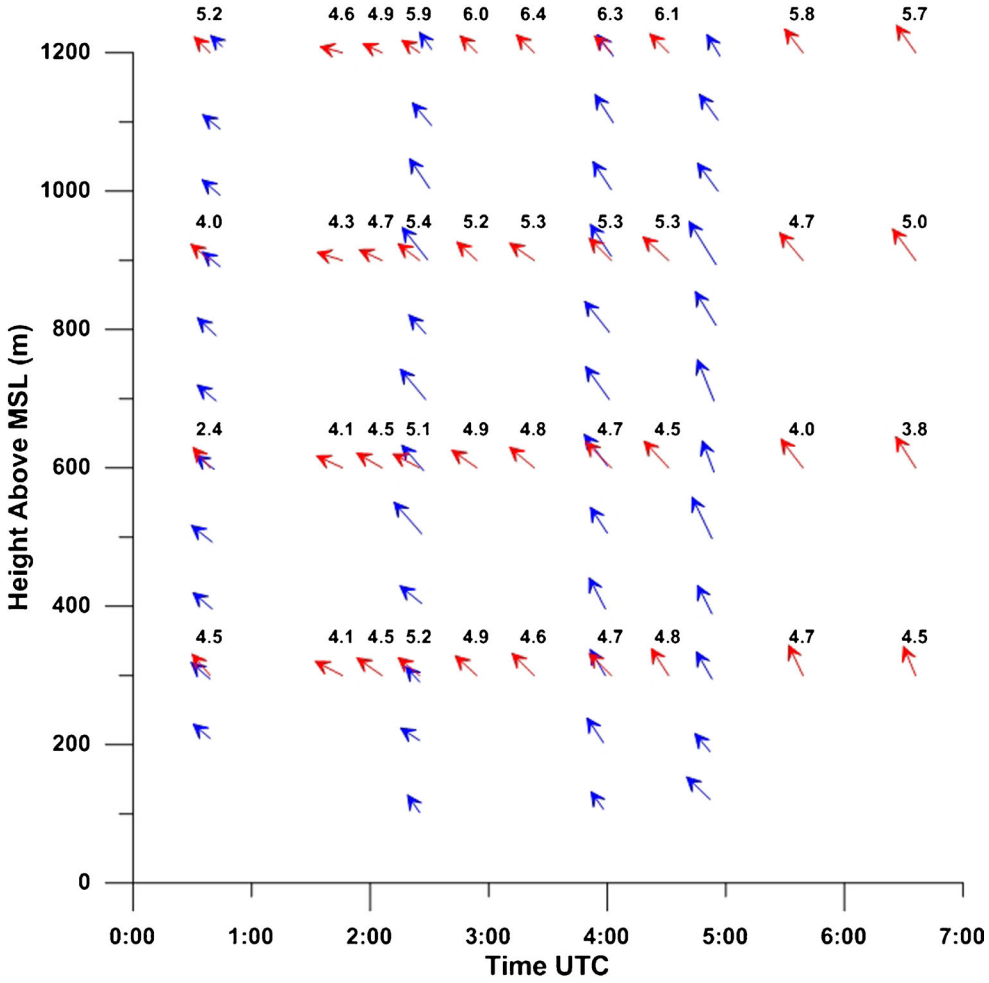

Fig. 10 Time-height cross-section of wind velocity (m s^{-1}) based on pilot balloon and rawinsonde measurements at Moore Air Base, Texas, (*red*) and WSR-88D CAPPI at Brownsville, Texas, (*blue*) on the night of 5–6 June 1996

of crop pest insects. Significant relationships between the aerial concentration of CEW and radar reflectivity were documented between ranges of 67–105 km from the nearest WSR-88D radar. Clear-air reflectivity maps indicated that the coverage may extend beyond a range of 180 km during peak migrations. Partial beam-filling will occur if insects are concentrated in layers or otherwise do not uniformly fill the radar beam, the likelihood of which increases with range from the radar. Additional insect concentration data should be obtained for regression with reflectivity to develop more robust relationships. Atmospheric refraction of the radar beam should be considered to accurately calculate the altitude of the radar beam and consequently of the targets that are reflecting electromagnetic energy back toward the WSR-88D radar (Barker 1994). In this study, we have found that clear-air radar reflectivity patterns caused by CEW and other similar-size insects was characterized by a rapid increase in reflectivity over agricultural areas during the 1st 1–2 h after sunset, followed by a steady decrease until sunrise. Reflectivity patterns associated with CEW moths became less concentrated as the moths flew away from the WSR-88D into areas of greater range interval volume.

WSR-88D CAPPI estimates of wind velocity were significantly correlated with wind velocity values measured by rawinsondes. Caution must be exercised in interpreting radar-estimated wind velocity values because CEW moths will affect the radar-estimated wind speed, and may affect the estimated wind direction. For example, weather forecasters often rely on radar measurements of wind velocity to detect low-level wind jets, wind shear, advection, and other wind profile features, but influences of the flight velocity of organisms may confound these values. Wind velocity values estimated from WSR-88D CAPPI wind velocity values combined with spectrum width values may be used to advect radar reflectivity values and estimate areawide insect dispersal for crop protection advisories.

Future research should include additional field measurements of atmospheric refractive index and wind velocity at additional bearing and range locations around the WSR-88D volume scan. Determining the identity, vertical distribution, aerial concentration, and flight behavior of insect species will enhance the value of agronomic information that can be derived from WSR-88D data products.

Acknowledgments P.D. Lingren initiated the collaboration between insect migration scientists and operational meteorologists for development of insect monitoring applications of the NEXRAD WSR-88D Doppler weather radar system. J.A. Lee and S. Fuller helped to install software, process data, and generate graphics. P.G. Schleider, E.C. Lawrence, A.A. Morrison, and J.A. Lee assisted with meteorological and radar entomological field operations. D. Priegnitz and L.R. Johnson explained the use of earlier versions of software to display WSR-88D data. S. Allen, J.D. Ward, N. Rydell, P. Yura, J. Snyder, and B. Read ensured that the requested radar scanning mode was operating when archiving WSR-88D radar data products during the field study. Mention of trade names or commercial products in this publication is solely for the purpose of providing specific information and does not imply recommendation or endorsement by the US Department of Agriculture. USDA is an equal opportunity provider and employer.

References

Achtemeier GL (1991) The use of insects as tracers for "clear-air" boundary-layer studies by Doppler radar. J Atmos Oceanic Technol 8:746–765

Barker T (1994) RDRHGT.EXE computer program. Western Regional Programming Note No. 109. USDC/NOAA/NWS, Missoula, MT

Beerwinkle KR, Witz JA, Schleider PG (1993) An automated, vertical looking, X-band radar system for continuously monitoring aerial insect activity. Trans Am Soc Agr Eng 36:965–970

Chapman JW, Reynolds DR, Smith AD (2003) Vertical-looking radar: a new tool for monitoring high-altitude insect migration. BioScience 53:503–511

Chapman JW, Nesbit RL, Burgin LE, Reynolds DR, Smith AD, Middleton DR, Hill JK (2010) Flight orientation behaviors promote optimal migration trajectories in high-flying insects. Science 327:682–685

Chapman JW, Drake VA, Reynolds DR (2011) Recent insights from radar studies of insect flight. Annu Rev Entomol 56:337–356

Chapman JW, Bell JR, Burgin LE, Reynolds DR, Pettersson LB, Hill JK, Bonsall MB, Thomas JA (2012) Seasonal migration to high latitudes results in major reproductive benefits in an insect. Proc Natl Acad Sci USA 109:14924–14929

Chilson PB, Bridge E, Frick WF, Chapman JW, Kelly JF (2012a) Radar aeroecology: exploring the movements of aerial fauna through radio-wave remote sensing. Biol Lett 8:698–701

Chilson PB, Frick W, Kelly J, Howard K, Kelly A, Diehl R, Larkin R, Westbrook J, Kunz T (2012b) Partly cloudy with a chance of migration: weather, radars, and aeroecology. Bull Am Meteorol Soc 93:669–686

Chilson PB, Frick WF, Stepanian PM, Shipley JR. Kunz TH, Kelly JF (2012c) Estimating animal densities in the aerosphere using weather radar: to Z or not to Z?, Ecosphere 3, article 72. doi:10.1890/ES12-00027.1

Crum TD, Alberty RL (1993) The WSR-88D and the WSR-88D operational support facility. Bull Am Meteorol Soc 74:1669–1687

Dean TJ, Drake VA (2005) Monitoring insect migration with radar: the ventral–aspect polarization pattern and its potential for target identification. Int J Rem Sens 26:3957–3974

Dokter A, Liechti F, Stark H, Delobbe L, Tabary P, Holleman I (2011) Bird migration flight altitudes studied by a network of operational weather radars. J R Soc Interface 8:30–43

Doviak RJ, Zrnic DS (1984) Doppler weather radar and weather observations. Academic, New York

Feng HQ, Zhao XC, Wu XF, Wu B, Wu K, Cheng DF, Guo YY (2008) Autumn migration of *Mythimna separata* (Lepidoptera: Noctuidae) over the Bohai Sea in Northern China. Environ Entomol 37:774–781

Feng H, Wu X, Wu B, Wu K (2009) Seasonal migration of *Helicoverpa armigera* (Lepidoptera: Noctuidae) over the Bohai Sea. J Econ Entomol 10:95–104

Gauthreaux SA Jr, Belser GG (1998) Displays of bird movements on the WSR-88D: patterns and quantification. Weather Forecast 13:453–464

Gauthreaux SA Jr, Mizrahi DS, Belser GG (1998) Bird migration and bias of WSR-88D: wind estimates. Weather Forecast 13:465–481

Hobbs SE, Aldhous AC (2006) Insect ventral radar cross-section polarization dependence measurements for radar entomology. IEE Proc-Radar Sonar Navig 153:502–508

Horn JW, Kunz TH (2008) Analyzing NEXRAD Doppler radar images to assess nightly dispersal patterns and population trends in Brazilian free-tailed bats (*Tadarida brasiliensis*). Integr Comp Biol 48:24–39

Jain M, Eilts M, Hondl K (1993) Observed differences of the horizontal wind derived from Doppler radar and a balloon-borne atmospheric sounding system. Preprints of the 8th Symposium on Meteorological Observations and Instrumentation, Anaheim, CA, American Meteorological Society, Boston, MA

Klazura GE, Imy DA (1993) A description of the initial set of analysis products available from the NEXRAD WSR-88D system. Bull Am Meteorol Soc 74:1293–1311

Larkin RP, Evans WR, Diehl RH (2002) Nocturnal flight calls of Dickcissels and Doppler radar echoes over South Texas in spring. J Field Ornithol 7:2–8

Miller PA, Barth MF, Smart JR, Benjamin LA (1997) The extent of bird contamination in the hourly winds measured by the NOAA Profiler Network: Results before and after implementation of the new bird contamination quality control check. Preprints of the 1st Symposium on Integrated Observing Systems, Long Beach, CA, American Meteorological Society, Boston, MA

Nieminen M, Leskinen M, Helenius J (2000) Doppler radar detection of exceptional mass-migration of aphids into Finland. Intl J Biometeor 44:172–181

NOAA (1990) Doppler radar meteorological observations; Part B: Doppler radar theory and meteorology (Interim Version One). US Department of Commerce, National Oceanic and Atmospheric Admininistration, Federal Meteorological Handbook Number 11

Orton R, Haddock DJ, Bice EG, Webb AC (1967) Climatic Guide: The Lower Rio Grande Valley of Texas. Texas Agricultural Experiment Station, College Station, TX, USA, Bulletin Number MP-841

Raulston JR, Pair SD, Loera J, Sparks AN, Wolf WW, Westbrook JK, Fitt GP, Rogers CE (1992) *Helicoverpa zea* (Lepidoptera: Noctuidae) pupa production in fruiting corn in northeast Mexico and south Texas. Environ Entomol 21:1393–1397

Rennie SJ, Dance SL, Illingworth AJ, Ballard SP, Simonin D (2011) 3D-Var assimilation of insect-derived Doppler radar radial winds in convective cases using a high resolution model. Mon Weather Rev 139:1148–1163

Reynolds DR (1988) Twenty years of radar entomology. Antenna 12:44–49

Riley JR (1985) Radar cross section of insects. Proc IEEE 73:228–232

Smith AD, Riley JR (1996) Signal processing in a novel radar system for monitoring insect migration. Comput Electron Agric 15:267–278

Westbrook JK, Eyster RS (2003) Nocturnal migrations of cotton insect pests indicated by Doppler radar observations. Proc Beltwide Cotton Conf, National Cotton Council, Memphis, TN, pp 997–1003

Westbrook JK, Wolf WW, Lingren PD, Raulston JR (1994) Tracking tetroons to evaluate budworm and bollworm migration. Proc Beltwide Cotton Conf, National Cotton Council, Memphis, TN, pp 791–793

Wilson JW, Weckwerth TM, Vivekanandan J, Wakimoto RM, Russell RW (1994) Boundary layer clear-air radar echoes: origin of echoes and accuracy of derived winds. J Atmos Oceanic Technol 11:1184–1206

Wolf WW, Westbrook JK, Sparks AN (1986) Relationship between radar entomological measurements and atmospheric structure in south Texas during March and April 1982. Long-range Migration of Moths of Agronomic Importance to the United States and Canada: Specific Examples of Occurrence and Synoptic Weather Patterns Conducive to Migration, A. N. Sparks, Ed., US Department of Agriculture, Washington, DC. Report ARS-43, pp 84–97

Wolf WW, Vaughn CR, Harris R, Loper GM (1993) Insect radar cross-sections for aerial density measurements and target classification. Trans Am Soc Agric Eng 36:949–954

Wolf WW, Westbrook JK, Raulston JR, Pair SD, Lingren PD (1995) Radar observations of orientation of noctuids migrating from corn fields in the Lower Rio Grande Valley. Southwestern Entomol Suppl 18:45–61

Wood CR, Chapman JW, Reynolds DR, Barlow JF, Smith AD, Woiwod IP (2006) The influence of the atmospheric boundary layer on nocturnal layers of noctuids and other moths migrating over southern Britain. Int J Biometeorol 50:193–204

Zrnic DS, Ryzhkov AV (1998a) Observations of insects and birds with a polarimetric radar. Geosci Rem Sens 36:661–668

Zrnic DS, Ryzhkov AV (1998b) Polarimetry for weather surveillance radars. Bull Am Meteorol Soc 80:389–406